

## THE TRACKING LINKAGE SYNTHESIS DESTINED TO DRIVE THE AZIMUTHAL MOTION FROM A PV TRACKER

Valentina POPA, Ion VISA, Dorin DIACONESCU,

Transilvania University of Braşov, Product Design for Sustainable Development Center,  
valentina.popa@unitbv.ro, visaion@unitbv.ro, dvdiaconescu@unitbv.ro

**Keywords:** tracking linkage, pressure angle, transmission angle, linkage synthesis, angular stroke.

**Abstract:** In the bi-axial tracking of a azimuthal tracked PV panel (aiming to maximize the normal direct solar radiation on PV panel), one of the two axes (with a large angular stroke:  $180^\circ \dots 360^\circ$ ) is usually driven by a gear speed reducer and the other axis (with a smaller angular stroke:  $\leq 90^\circ$ ) is driven by a triangle linear actuator linkage. Because a linear actuator is more economical than a rotary one, the paper reports on the use of linear actuators for the large angular strokes; this aim is fulfilled by the synthesis of a linkage consisting of two simple linkages, serially connected: a triangle linkage with a linear actuator and a four-bar linkage which amplifies the output angle of the first linkage up to about  $180^\circ$ .

### 1. INTRODUCTION

The PV tracking, single or bi-axial, is used for maximizing the normal incident direct solar radiation on the PV panels; thus a 20%...50% increase in the energetic efficiency can be achieved [5].

Bi-axial PV tracking systems of azimuthal type is mostly used [5]; one axis has a maximum  $90^\circ$  angular stroke (type I) and the other one has an angular stroke much more beyond this limit (type II).

The PV panel tracking by an axis of type I implies driving a revolute joint, materializing this axis, by a deformable triangle linkage which has the deformable side consisting in an electrical linear actuator. The tracking by an axis of type II supposes driving a revolute joint by a worm speed reducer or other gear reducer with a high speed ratio; unlike the tracking with a deformable triangle linkage, the tracking by a gear reducer ensures larger angular strokes, but has significant technical and economical disadvantages: higher technological cost, higher complexity, difficulties in reducing the backlashes and assuring the stability, lower efficiency in the case of the worm speed reducer.

Consequently, there were developed systems that extend the use of the deformable triangle linkage for the axis of type II; in this case, a reduction of the angular stroke (usually to about  $120^\circ$ - $140^\circ$ ), due to the pressure angles limitation [4] is expected.

The paper solves the problem of *the angular stroke increase, using a linear actuator*, by the synthesis of a linkage composed of two simple linkages, serially connected: a triangle linkage with a linear actuator and a four-bar linkage which amplifies the output angle of the first linkage up to about  $180^\circ$ .

### 2. SYNTHESIS INPUT DATA

In the azimuthal bi-axial tracking of the PV panels, there is used *the azimuthal angular system* (Fig.1) which interferes in the modelling of the current angular position of the sun-ray and the structure of the open kinematical chains (OKC) of the tracking linkages (see Fig.1 and 2): *azimuth*  $\psi$  and *altitude*  $\alpha$ ; the bi-mobile OKC, resulted by serial connection of the 2 rotations in the given order is named *azimuthal* OKC and is the most frequently used.

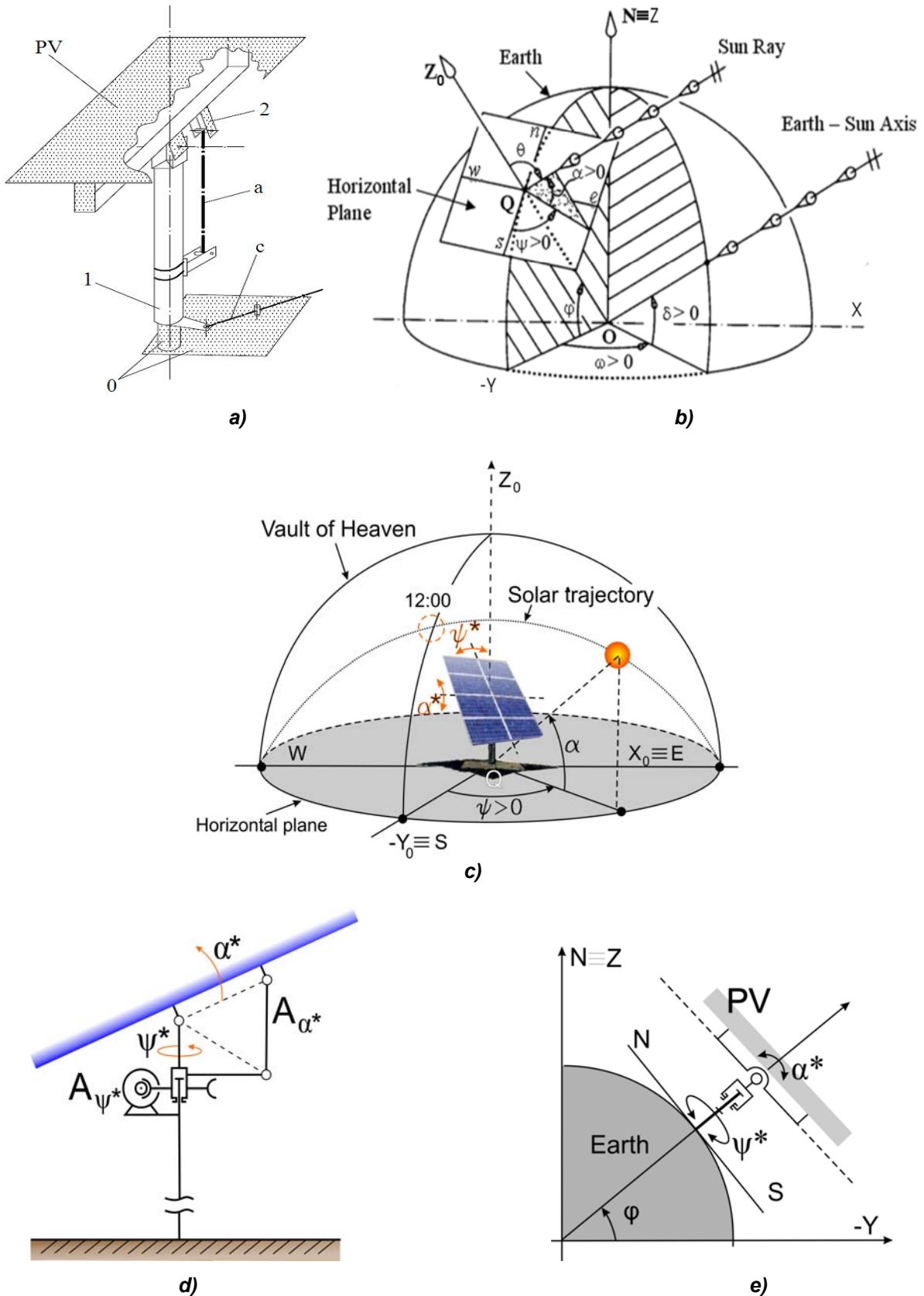


Fig. 1. a) A bi-axial azimuthal tracker with linear actuators; b and c) Sun-ray angles; d) Axes and actuators of the azimuthal trackers; e) Relative position of the tracker vs. Earth.

The sun-ray angles, presented correlation (1), ..., (7), are based on the correlations of the angles  $\omega$  and  $\delta$ , considered as primary input data [2; 3]:

$$\delta = 23.45^\circ \cdot \sin\left[360 \cdot \frac{N-80}{365}\right]; \quad \omega = 15^\circ \cdot (12-T); \quad (1); (2)$$

$$\sin \alpha = \sin \delta \cdot \cos \varphi + \cos \delta \cdot \cos \varphi \cdot \cos \omega; \quad \psi = (\text{sgn } \omega) \cdot \cos^{-1} \frac{\sin \alpha \cdot \sin \varphi - \sin \delta}{\cos \alpha \cdot \cos \varphi}; \quad (3); (4)$$

$$\cos v = \cos \alpha \cdot \cos \alpha^* \cdot \cos(\psi - \psi^*) + \sin \alpha \cdot \sin \alpha^*; \quad (5)$$

$$R_d = 1367 \cdot [1 + 0,0334 \cdot \cos(0,9856^\circ \cdot N - 2,72^\circ)] \cdot e^{\left(\frac{T_R}{0,9+9,4 \cdot s\alpha}\right)}; \quad (6)$$

$$R_{dr} = R_d \cdot \cos v; \quad (7)$$

where:  $\varphi$  – latitude;  $\delta$  – declination;  $\omega$  – hour angle;  $N$  – day number;  $T$  – solar time;  $\alpha$  - altitude;  $\psi$  – azimuth;  $v$  – incidence angle;  $\psi^*$ ,  $\alpha^*$ - tracker's angles;  $R_d$  – direct solar radiation;  $R_{dr}$  – direct solar radiation which falls normal on the PV panel;  $T_R$  – lost radiation factor.

The angular displacement of the tracked PV panel is made discreet (stepwise); to distinguish them from the sun-ray angles (which have continuous variations), in the correlations presented in this paper the tracker's angles are marked with asterisk:  $\psi^*$ ,  $\alpha^*$ .

Fig.2 presents the variation of the above angles during the Summer Solstice for the Braşov-Romania latitude ( $45.5^\circ$  N). According to Fig.2a, the daily angular stroke of the sun-ray is about  $250^\circ$  for  $\psi$ .

Considering certain stepped variations of the angles  $\psi^*$ ,  $\alpha^*$  and using the resulted incidence angle ((1), ..., (7)), the available solar direct radiation (the outer curve from the Fig.2b) and the received direct solar radiation that falls normal on the PV panel (the inner curve from the Fig.2b) can be established. Supposing that the whole day is cloudless, the area under the inner curve (Fig.2b) represents the energy of the direct solar radiation that falls normal on one square meter of PV panel.

For the existing tracking system, the angular movement corresponding to the  $\alpha^*$  angle has a reduce stroke (frequently  $\leq 90^\circ$ ) and is driven by a linear actuator; unlike this case, the angular movement corresponding to the  $\psi^*$  angle (with an angular strokes that can be over  $180^\circ$ ) is made usually with a rotary actuator, *which is usually less economically efficient than a linear actuator*. The use extension of the linear actuators for the angular movements correspondent to and  $\psi^*$  angle is exemplified in the Fig.1a, where the linear actuators are represented by dot-dash lines segments.

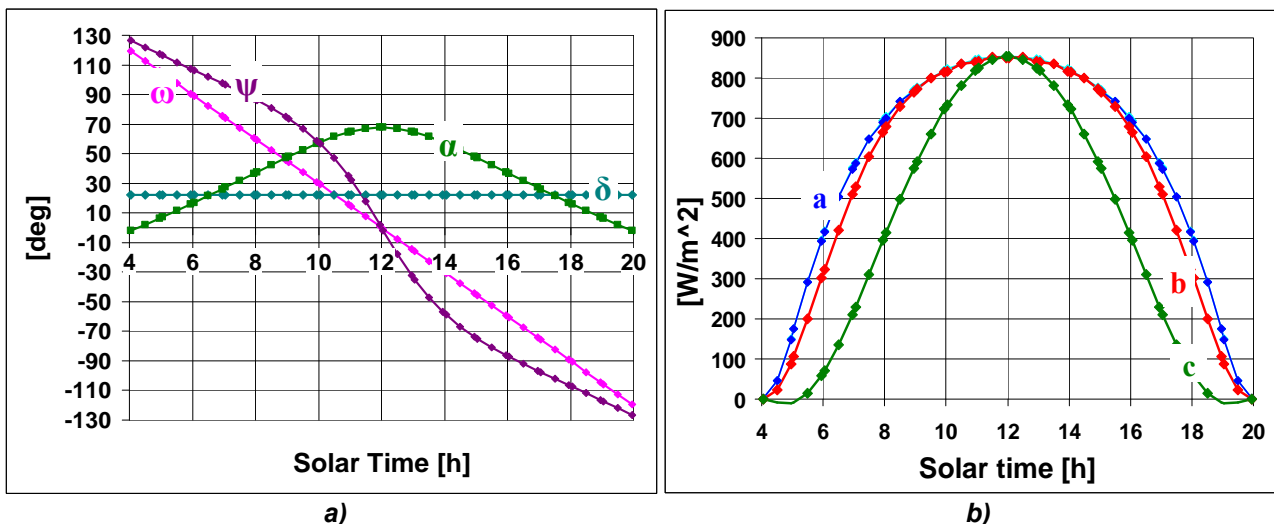


Fig. 2. Summer Solstice variations at  $45.5^\circ$ N correspondent to: a) the sun-ray angles; b) the direct solar radiation (a=available, b=tracked panel, c=fixed and tilted panel)

The driving of the azimuthal motion using a triangle linkage with a linear actuator (Fig.1a) reduces the tracking angular stroke due to the excessive increase of the pressure angle; this effect results from Fig.3:

a) Fig.3a shows that in a current position ABC (characterised by a pressure angle  $\beta_B$ ), the balance of the resistant moment  $T = F \cdot AB$  compels the actuator to produce a force:  $F_a = F \cdot (1/\cos\beta_B)$ ; the variation of the amplification factor  $1/\cos\beta_B = F_a/F$ , (Fig.3b) confirms that the limitation of the pressure angle maximum value to  $60^\circ$ ,  $70^\circ$  or  $80^\circ$  determines a 2, 3 and, respectively, 6 times force amplification.

b) Fig.3a also shows that the extreme values of  $\beta_{Bi}$  and  $\beta_{Bf}$  (corresponding to the pressure angle  $\beta_B$  at the margins of the angular stroke  $B_iAB_f$ ) become equal in their absolute values if the points C,  $B_i$  and  $B_f$  are collinear; in this case, the maximum value of the pressure angle equals the half of the angular stroke  $B_iAB_f$  (Fig.3a) and, consequently, the angular stroke becomes  $B_iAB_f = 2 \cdot \beta_{B,\max. \text{ admitted}} \approx 120^\circ \dots 140^\circ$ ; increasing the angular stroke beyond these values can have negative consequences on the resistance and the stability of the tracking linkage.

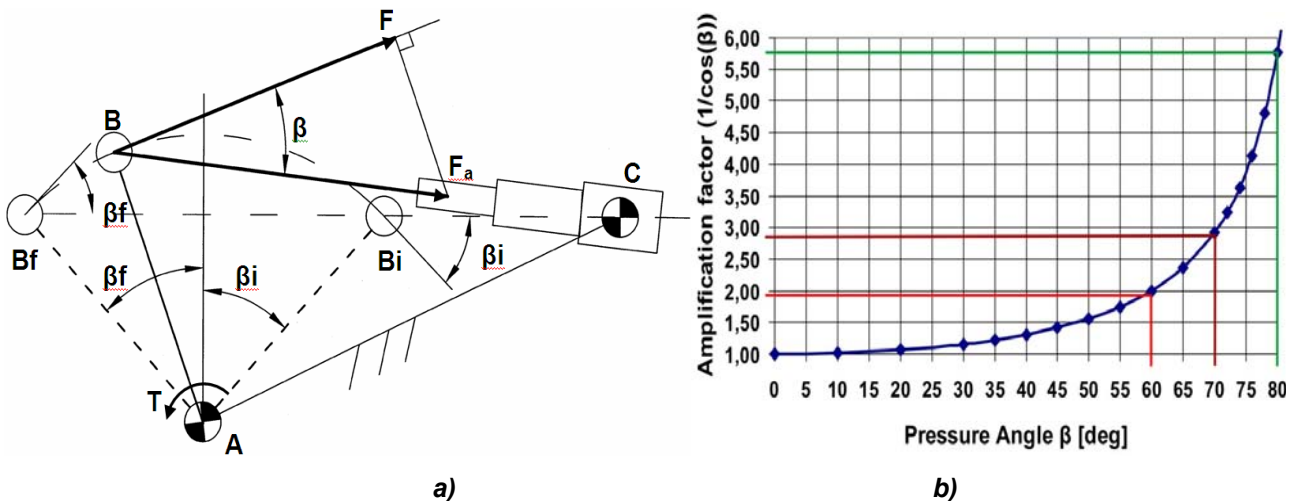


Fig. 3. a) The scheme of the triangle linkage with a linear actuator; b) The variation of the amplification factor depending on the pressure angle.

Further, the problem of the angular stroke increase is solved, based on the use of a linear actuator; this solving consists in the synthesis of a linkage consisting in two simple linkages which are serially connected: a triangle linkage with a linear actuator (Fig.3a) and a four-bar linkage which amplifies the output angle of the first linkage up to  $180^\circ$ ; obviously, the accent will be on the synthesis of the angular amplifier linkage.

### 3. TRACKING LINKAGE SYNTHESIS

The synthesis of the conceptual solutions of the linkage with linear actuator for reaching an  $180^\circ$  angular stroke is presented in Fig.4 and has the following formulation: using a triangle linkage with a linear actuator, an angular stroke about  $90^\circ$  is applied to a rocker; this angular stroke is then amplified to  $180^\circ$  by a four-bar linkage; the requirement is to establish the reduced dimensions (related to the length of one of the elements) of the four-bar linkage elements, considering that the maximum admissible pressure angle is  $60^\circ$  (consequently, the minimum admissible transmission angle is  $90^\circ - 60^\circ = 30^\circ$ ).

The synthesis is graphically presented in the Fig.4a:

- 1) the little rocker AB (with angular stroke of  $180^\circ$ ) is traced in the extreme positions  $AB_i$  and  $AB_f$ ; its length is considered as unit (1);

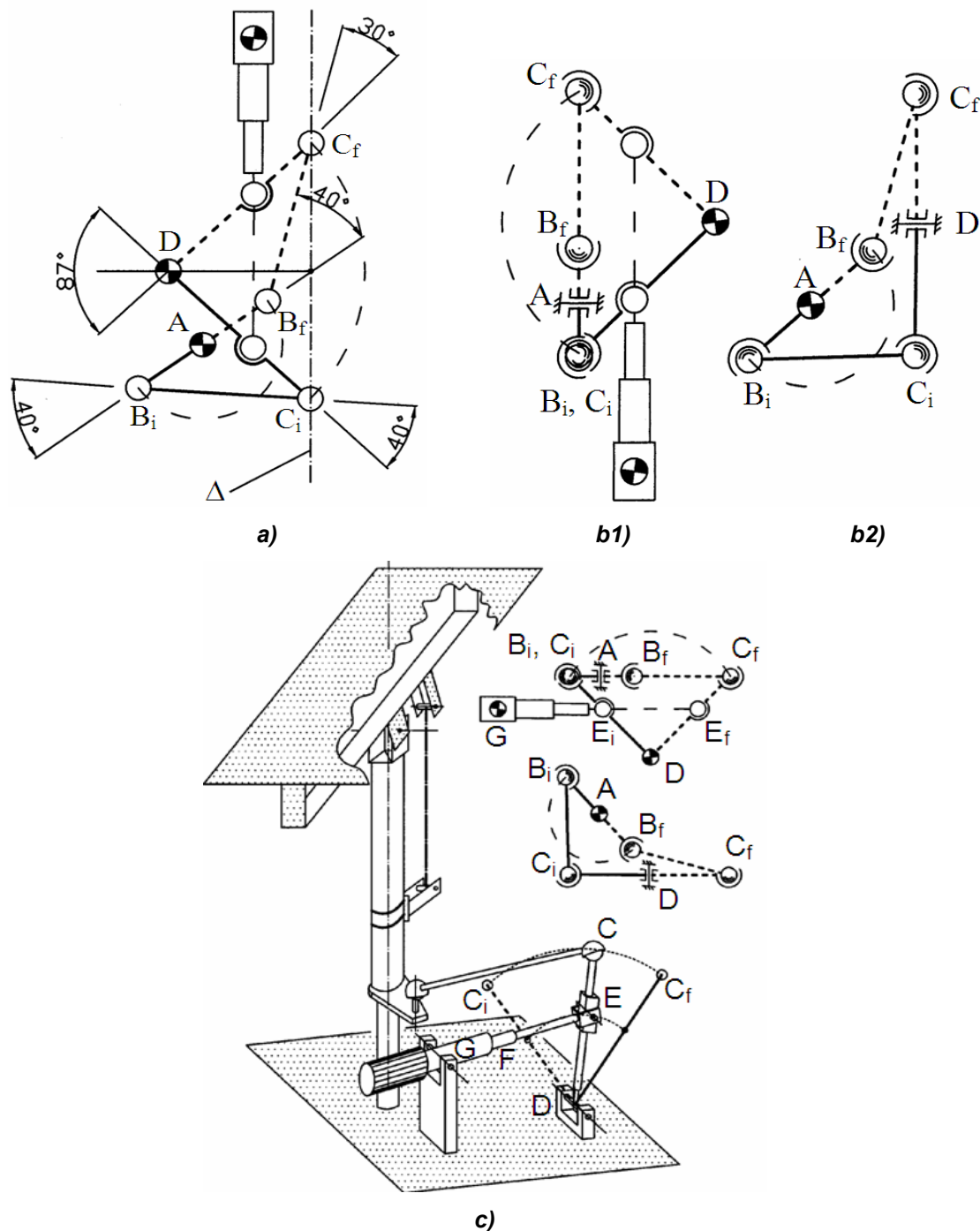


**Fig. 4. Two solutions of the four-bar linkage synthesis:**  
*a) plane solution; b<sub>1</sub>+ b<sub>2</sub>) spatial solution; c) an application of the spatial solution.*

- 2) for improved stability, the connecting rod extreme positions  $B_iC_i$  and  $B_fC_f$  are traced, so that the connecting rod and the little rocker form a  $40^\circ$  transmission angle; the connecting rod length is chosen as little as possible, but considering that in the initial position, the rocker  $C_iD$  will not interfere with the revolute joint  $A$ ;
- 3) then, there are traced: the line  $\Delta$  through the points  $C_i$  and  $C_f$  and the median perpendicular of  $C_iC_f$ , which contains the joint centre  $D$  of the big rocker; the point  $D$  is chosen so that between the connecting rod ( $B_fC_f$ ) and the rocker  $C_fD$  a transmission angle of  $30^\circ$  is formed; thus (see Fig.4a), result the reduced dimensions

of the connecting rod BC ( $BC/AB = 2.1694$ ), of the rocker CD ( $CD/AB = 2.4742$ ) and of the base DA ( $DA/AB = 1.0714$ );

- 4) a linear actuator (articulated at base) is attached to the big rocker (CD), analogous to Fig.4a;
- 5) by turning with  $90^\circ$  the triangle  $C_1C_1D$  from Fig.4a, around the line  $\Delta$ , the spatial solution from Fig.4b<sub>1</sub> and 4b<sub>2</sub> is obtained; in this situation the configuration of the AD base changes and is described using the following reduced dimensions (Fig.4b<sub>1</sub> and 4b<sub>2</sub>): the distance between the axes A and D ( $AD/AB=0.9778$ ); the distance from the vertical articulation A to the vertical median plane of the rocker CD: 1.3542; the distance from the horizontal articulation D to the horizontal median plane of the AB element: 1.7922.

Fig.4c represents an application of the linkage from Fig.4b<sub>1</sub> and 4b<sub>2</sub>, in an azimuthal tracker, for the movement  $\psi^*$  driving.

For the applications of the plane linkage and the spatial linkage (Fig.4a, 4b1 and 4b2), Fig.5 and Fig.6 show the relevant positions and the specific geometrical parameters, along with the variations of the pressure angles  $\beta_B$ ,  $\beta_C$  and of the angular displacement  $\Phi$ , depending on the angular displacement  $\psi^*$ . These graphical correlations were validated using the MBS (Multi-Body Systems) Method [1].

Firstly the transmission angles were determined and afterwards the pressure angles were established as the  $90^\circ$  complements of the transmission angles.

For the considered positions of the plane linkage, the transmission angles were measured using the Catia software.

For the considered positions of the spatial linkage, by means of the triangle metric relations, the following side measures were obtained (see Fig.5c):

$$AC = \sqrt{a^2 + b^2}; BC = \sqrt{e^2 + b^2}; BD = \sqrt{d^2 + c^2}; \quad (8); (9); (10)$$

where AC is the side which closes the triangle ABC formed by the little rocker AB and the connecting rod BC and BD is the side which closes the triangle BCD formed by the connecting rod BC and the big rocker CD.

The transmission angles  $\gamma_B$  (between the little rocker AB and the connecting rod BC) and  $\gamma_C$  (between the big rocker CD and the connecting rod BC), can be obtained from the triangle ABC and, respectively, the triangle BCD (Fig.5c):

$$\cos \gamma_B = \frac{BC^2 + AB^2 - AC^2}{-2 * AB * BC}; \cos \gamma_C = \frac{BC^2 + CD^2 - BD^2}{2 * BC * CD}; \quad (11); (12)$$

where for the elements AB, BC and CD were considered the reduced dimensions:  $AB=1$ ,  $BC = 2.1694$  and  $CD = 2.4742$ . In accordance with Fig.6, the differences between the homologous sizes of the two linkages are relatively small.

#### 4. CONCLUSIONS

a) A gear speed reducer ensures very large angular strokes, but is less economical than a rotary linkage with a linear actuator; yet, the use of a simple triangle linkage with linear actuator reduces the angular stroke of the tracking axis, due to the pressure angle limitation (the maximal angular strokes are usually limited at  $120^\circ$ - $140^\circ$ ).

b) The increase of the angular stroke, considering a linear actuator, is presented in the paper by synthesis of a linkage consisting in two simple linkages which are serially connected: a triangle linkage with a linear actuator (Fig.4a) and a four-bar linkage which *amplifies* the output angle of the first linkage up to  $180^\circ$ .

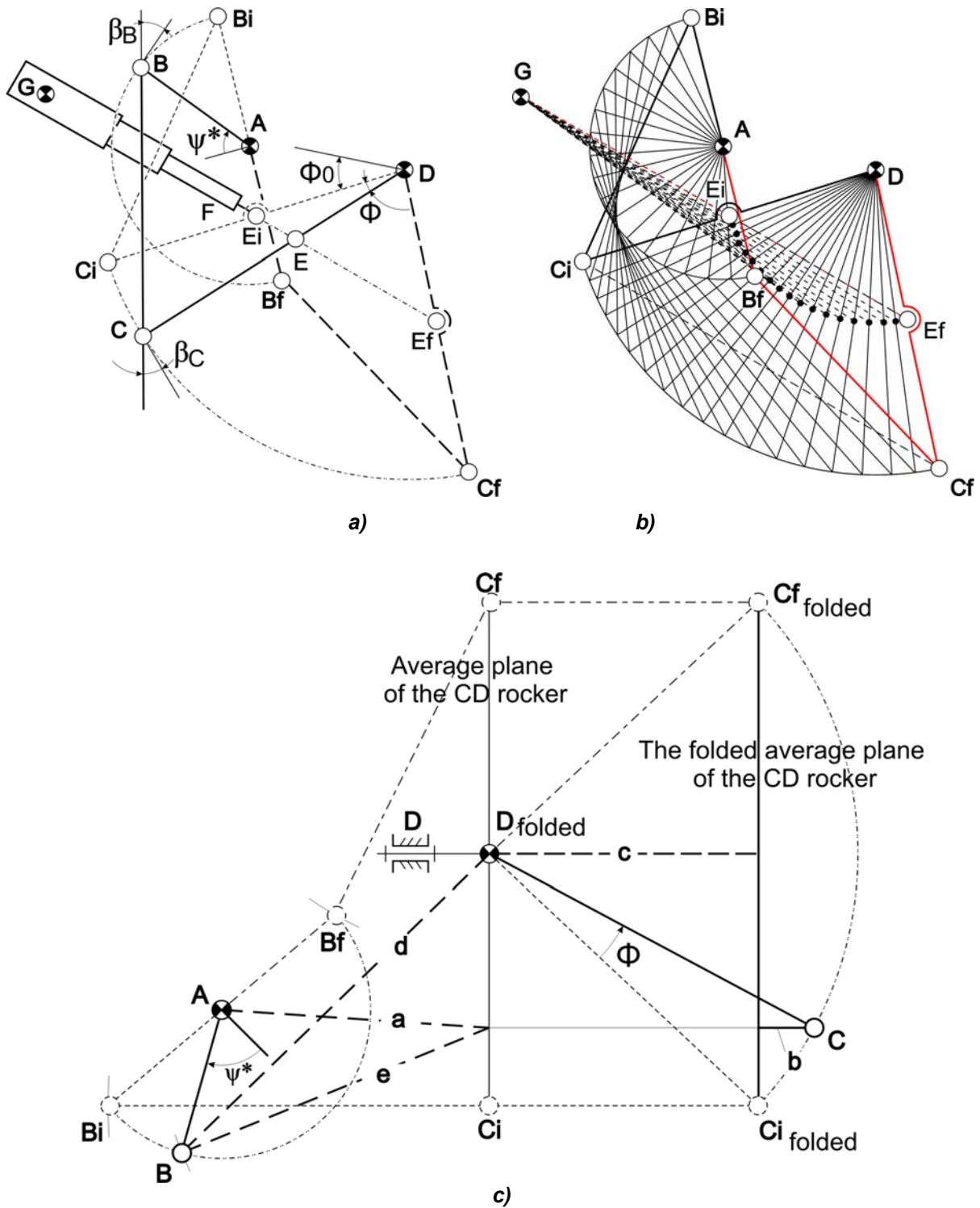
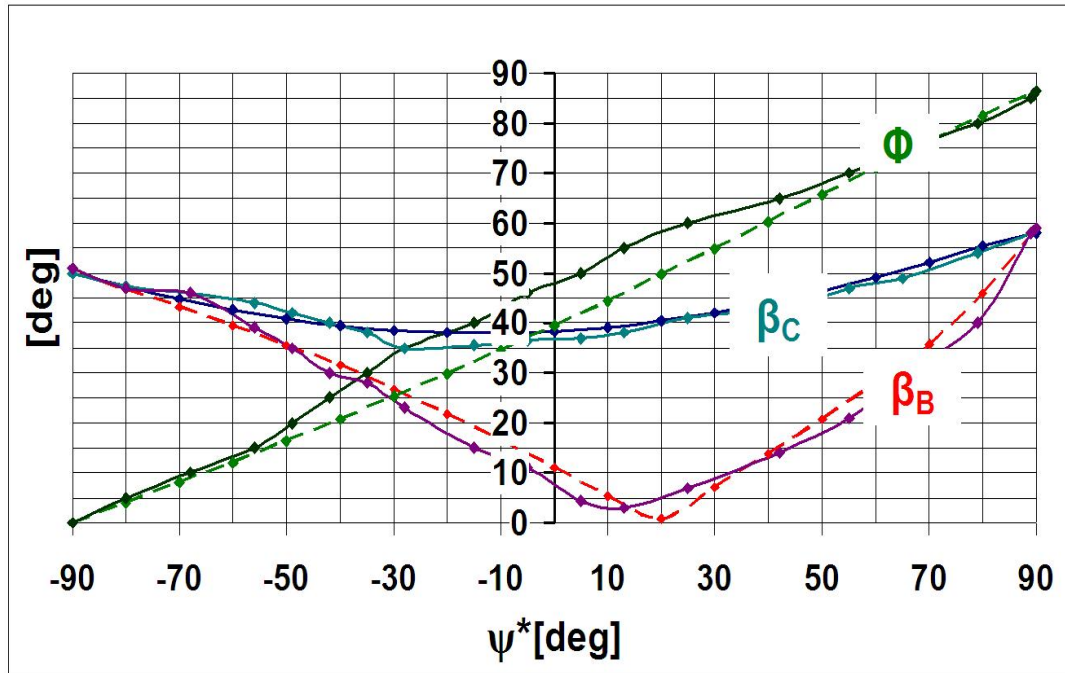


Fig. 5: a) The current and extreme positions of the plane linkage (see Fig.4); b) Successive positions of the plane linkage; c) The current and extreme positions of the spatial linkage (in which: a-the AC projection on the  $BiABf$  plane; d-the BD projection on the  $BiABf$  plane; e-the BC projection on the  $BiABf$  plane)

c) By the above synthesis, two conceptual solutions were generated for an *angular amplifier*, applicable in tracking the solar PV panels: a planar solution and a spatial solution (Fig.4); in accordance with Fig.6, the differences between the homologous sizes of the two linkages are relative small.



**Fig. 6.** The variations of the pressure angle  $\beta_B$ ,  $\beta_C$ , and of the angular displacement  $\Phi$  depending on the angle  $\psi^*$  (the continuous curves belong to the spatial linkage and the dot-dash curves belong to the plane linkage)

## REFERENCES

- [1] Haug J.E., *Computer Aided Kinematics and Dynamics of mechanical Systems*, Allyn and Bacon, USA, 1989.
- [2] Messenger R., Ventre J., *Photovoltaic System Engineering*, CRC Press, London, 2000.
- [3] Visa, I., Diaconescu, D., Popa, V., Burduhos, B., Saulescu R., *The Synthesis of a Linkage with Liner Actuator for Solar Tracking with Large Angular Stroke*, 2-nd European Conference on Mechanism Science EUCOMES 2008, 17- 20 September 2008: Cassino , Italy (accepted by the scientific committee)
- [4] Norton, R.L., *Design of machinery*, Mc Graw Hill, Boston, 1999.
- [5] [www.wattsun.com](http://www.wattsun.com) , [www.lorentz.com](http://www.lorentz.com) , [www.deger.de](http://www.deger.de)